JCTC Journal of Chemical Theory and Computation

A Molecular Energy Decomposition Scheme for Atoms in Molecules

E. Francisco,* A. Martín Pendás, and M. A. Blanco

Departamento de Química Física y Analítica, Facultad de Química, Universidad de Oviedo, 33006-Oviedo, Spain

Received September 5, 2005

Abstract: An exact energy partition method based on a physically sound decomposition of the nondiagonal first-order and diagonal second-order density matrices put forward by Li and Parr (*J. Chem. Phys.* **1986**, *84*, 1704) is presented. The method splits the total energy into intra- and interatomic components and is applicable on quite general wave functions. To explore it numerically, the energy components of three test molecules (H_2, N_2, and LiH) have been computed using four different partitions of the charge density $\rho(\mathbf{r})$ into atomic densities. Several aspects on the chemical bond and the relative importance of different components of the binding energy are analyzed. The merits of different partitions of $\rho(\mathbf{r})$ are also discussed.

I. Introduction

Chemists usually see molecules as formed by atoms or groups of atoms interacting with each other in 3D space and approximately having transferable properties. This idea has inspired the translation of the well-known concepts of chemistry such as bonds, valences, atomic charges, and so forth to the quantum mechanical language. In looking for this connection, the proposed models usually start at a qualitative level, but as soon as they slide into the quantitative realm, they fall into a fragment picture. Many of these quantitative models try, then, energy partition schemes or energy decomposition analyses.[1−22]

All of these methods, which have importantly contributed to deepening our knowledge of the chemical bond, are not free from criticisms. A number of them are (a) their link to particular calculational procedures, (b) their dependence on the reference used to describe the fragments, (c) their use of fictitious intermediate states, and (d) their mixing of exchange and orthogonality constraints.

Recently, we presented an energy partition method that is theoretically sound and able to give detailed definitions of the interactions among atoms, functional groups, and molecules.[23] Moreover, it is exhaustive in the sense that it recovers exactly the total energy of the system and derives from the molecular wave function without resorting to the approximations involved in its calculation. Its implementation was possible thanks to the previous development of an efficient algorithm to compute two-electron integrals over arbitrary regions of space for both monodeterminantal[24] and correlated[25] wave functions. In ref 23, the atomic regions of the quantum theory of atoms in molecules (QTAM), mainly developed by Bader,[11] were taken as basic entities from which the molecule is built. The QTAM atoms, unequivocally defined as the 3D attraction basins of the gradient field of the molecular charge density $\rho(\mathbf{r})$, have sharp and well-defined boundaries and, thus, produce noninterpenetrating atomic densities. Their irregular forms and the high computational cost which is necessary to determine their boundaries has prevented their wide use in routine quantum chemical applications. For this reason, the objective of this paper is to present a molecular energy decomposition scheme that, taking also the individual atoms as the chemically meaningful fragments in the molecule, generalizes the earlier one based on QTAM atoms.[23] The basic idea of the generalized approach is to partition $\rho(\mathbf{r})$ in terms of interpenetrating atomic densities $\rho_A(\mathbf{r})$ that have no defined boundaries. The charge density at any point of physical space is not assigned to a single atom as in QTAM but is shared to a certain degree by all the atoms of the molecule. Since each $\rho_A(\mathbf{r})$ extends to infinity, the obstacles associated with the steplike character of QTAM atoms clearly disappear and

* Corresponding author. Phone: +34 985103039. E-mail: evelio@carbono.quimica.uniovi.es.

10.1021/ct0502209 CCC: $33.50
Published on Web 12/02/2005

the task of determining atomic boundaries is obviously absent. The only requisite that the $\rho_A(\mathbf{r})$ has to satisfy is

$$\rho(\mathbf{r}) = \sum_A w_A(\mathbf{r})\,\rho(\mathbf{r}) = \sum_A \rho_A(\mathbf{r}) \tag{1}$$

where the $w_A(\mathbf{r})$ functions provide a partition of the unity

$$\sum_A w_A(\mathbf{r}) = 1\ \forall \mathbf{r} \tag{2}$$

A partition of $\rho(\mathbf{r})$ into atomic components does not unequivocally define a corresponding energy partition since the total energy depends not only on $\rho(\mathbf{r})$ but also on the nondiagonal part of the first-order density matrix, $\rho_1(\mathbf{r},\mathbf{r}')$, and the diagonal second-order density matrix, $\rho_2(\mathbf{r}_1,\mathbf{r}_2)$. Consequently, a second and essential step in the energetic partition that we propose is to convey the partition of $\rho(\mathbf{r})$ to the full nondiagonal density matrices from which the total energy depends. This should be done, in our opinion, using physically reasonable arguments. We will use, in this article, the scheme proposed in the 1980s by Li and Parr.[26] It is very relevant to remark that Li and Parr's scheme allows for a physically sound partition of $\rho_1(\mathbf{r},\mathbf{r}')$ and $\rho_2(\mathbf{r}_1,\mathbf{r}_2)$ only in terms of a given partition of $\rho(\mathbf{r})$.

The third and last step in our partition method is to group or reorganize the different energy components into physically and chemically meaningful contributions. Altogether, these three elements represent a practical and physically well-founded methodology to partition the total energy, energy components, and density matrices into intra-atomic and interatomic terms. As we will see below, the algorithm works equally well with very different and unconnected partitions of $\rho(\mathbf{r})$: interpenetrating (in both its localized and delocalized versions) and noninterpenetrating (in which the atomic densities are exactly zero outside a given 3D region).

We have organized the rest of the paper as follows. In Section II, we present the energy partition method. In Section III, we present and discuss the results. First, taking the CO molecule as a test example, we analyze its atomic charges and densities and discuss the results found for these properties in other molecules (Subsection IIIA). Then, we perform a thorough comparative study of the energy components in H_2 using four possible partitions of $\rho(\mathbf{r})$ and show how their relative values are governed by the hydrogen atomic density in each of the partitions (Subsection IIIB). Similar studies on the N_2 and LiH molecules (representative of the traditional apolar covalent and partially ionic bonding types, respectively) are presented in Subsections IIIC and IIID, respectively. Finally, a summary and our conclusions are given in Section IV.

II. Energy and Charge Density Partitions

In this section, we present some theoretical aspects of the energy partition method that we propose (Subsection IIA), show how the different energy components can be rearranged to obtain deeper insights into their physical meaning (Subsection IIB), define the partitions of the charge density into atomic densities with which the energy partition has actually been applied (Subsection IIC), and give some relevant computational details concerning the practical evaluation of all the energy components (Subsection IID).

A. Energy Partition. Since the nonrelativistic Born−Oppenheimer molecular Hamiltonian contains only one- and two-particle terms, the total energy of a molecule may be obtained from just the spin-free first order, $\rho_1(\mathbf{r},\mathbf{r}')$, and diagonal second order, $\rho_2(\mathbf{r}_1,\mathbf{r}_2)$, reduced density matrices as[27]

$$E = E_e + V_{nn} = (T + V_{ne} + V_{ee}) + V_{nn} \tag{3}$$

where

$$T = \int_{\mathbf{r}'\to\mathbf{r}} \hat{T}\rho_1(\mathbf{r},\mathbf{r}')\,d\mathbf{r} \tag{4}$$

$$V_{ne} = -\sum_A Z_A \int \frac{\rho(\mathbf{r})}{|\mathbf{r}-\mathbf{R}_A|}\,d\mathbf{r} \tag{5}$$

$$V_{ee} = \frac{1}{2}\int \frac{\rho_2(\mathbf{r}_1,\mathbf{r}_2)}{r_{12}}\,d\mathbf{r}_1\,d\mathbf{r}_2 \tag{6}$$

and

$$V_{nn} = \frac{1}{2}\sum_A\sum_{B\neq A} V_{nn}^{AB} = \frac{1}{2}\sum_A\sum_{B\neq A}\frac{Z_A Z_B}{R_{AB}} \tag{7}$$

are the total kinetic energy, nucleus−electron attractive potential energy, electron−electron repulsion energy, and nuclei−nuclei repulsion energy, respectively, $\hat{T} = {}^1/_2\nabla\cdot\nabla'$, and $\rho(\mathbf{r}) \equiv \rho_1(\mathbf{r},\mathbf{r})$. What we want is a consistent partition of $\rho_1(\mathbf{r},\mathbf{r}')$ and $\rho_2(\mathbf{r}_1,\mathbf{r}_2)$ (and from it, a partition of the total energy) using exclusively a well-defined partition of $\rho(\mathbf{r})$ into atomic densities $\rho_A(\mathbf{r})$'s. A method to do this was proposed 20 years ago by Li and Parr.[26] Following these authors, we assume the validity of eq 1 also for the nondiagonal $\rho_1(\mathbf{r},\mathbf{r}')$ and partition it in the form

$$\rho_1(\mathbf{r},\mathbf{r}') = \sum_A w_A(\mathbf{r}')\,\rho_1(\mathbf{r},\mathbf{r}') = \sum_A \rho_1^A(\mathbf{r},\mathbf{r}') \tag{8}$$

where the $w_A(\mathbf{r})$'s satisfy eq 2. It may then be shown that

$$\left.\frac{\hat{T}\rho_1^A(\mathbf{r},\mathbf{r}')}{\rho_1^A(\mathbf{r},\mathbf{r}')}\right|_{\mathbf{r}'\to\mathbf{r}} = \left.\frac{\hat{T}\rho_1(\mathbf{r},\mathbf{r}')}{\rho_1(\mathbf{r},\mathbf{r}')}\right|_{\mathbf{r}'\to\mathbf{r}} \quad \forall A \tag{9}$$

In Li and Parr's original scheme, based on density functional theory (DFT), this amounts, to scale, the exact kinetic density functional. A very similar scaling is done to partition $\rho_2(\mathbf{r}_1,\mathbf{r}_2)$, this time, with a double scaling for electrons 1 and 2:

$$\rho_2(\mathbf{r}_1,\mathbf{r}_2) = \sum_A\sum_B w_A(\mathbf{r}_1)\,w_B(\mathbf{r}_2)\,\rho_2(\mathbf{r}_1,\mathbf{r}_2) \tag{10}$$

$$= \sum_A\sum_B \rho_2^{AB}(\mathbf{r}_1,\mathbf{r}_2) \tag{11}$$

This partition implies that

$$\frac{\rho_2^{AA}(\mathbf{r}_1,\mathbf{r}_2)}{\rho_A(\mathbf{r}_1)\,\rho_A(\mathbf{r}_2)} = \frac{\rho_2^{AB}(\mathbf{r}_1,\mathbf{r}_2)}{\rho_A(\mathbf{r}_1)\,\rho_B(\mathbf{r}_2)} = \frac{\rho_2(\mathbf{r}_1,\mathbf{r}_2)}{\rho(\mathbf{r}_1)\,\rho(\mathbf{r}_2)} \tag{12}$$

which means that, given two arbitrary points $\mathbf{r}_1$ and $\mathbf{r}_2$, the interaction energy between two electrons is the same no matter whether we assume them as belonging to an atom or to the molecule.

These ideas lead to a partition of all the energy components into intra- and interatomic contributions. For instance, using eqs 2 and 8 in eq 4, we obtain

$$T = \sum_A T^A = \sum_A \int_{\mathbf{r}'\to\mathbf{r}} w_A(\mathbf{r})\, \hat{T}\rho_1(\mathbf{r},\mathbf{r}')\, d\mathbf{r} \tag{13}$$

Similarly, when eq 1 is used in eq 5, V_{ne} is given as

$$V_{ne} = -\sum_A \sum_B Z_A \int \frac{\rho_B(\mathbf{r})}{|\mathbf{r}-\mathbf{R}_A|}\, d\mathbf{r} = \sum_A \sum_B V_{ne}^{AB} \tag{14}$$

Finally, inserting eq 11 in eq 6, V_{ee} results:

$$V_{ee} = \sum_A V_{ee}^{AA} + \frac{1}{2}\sum_A \sum_{B\neq A} V_{ee}^{AB} \tag{15}$$

where

$$V_{ee}^{AA} = \frac{1}{2}\int \frac{\rho_2^{AA}(\mathbf{r}_1,\mathbf{r}_2)}{r_{12}}\, d\mathbf{r}_1\, d\mathbf{r}_2 \tag{16}$$

and

$$V_{ee}^{AB} = \int \frac{\rho_2^{AB}(\mathbf{r}_1,\mathbf{r}_2)}{r_{12}}\, d\mathbf{r}_1\, d\mathbf{r}_2 \tag{17}$$

Inserting now eqs 7, 13, 14, and 15 in eq 3, the total energy can be expressed as

$$E = \sum_A E_{net}^A + \frac{1}{2}\sum_A \sum_{B\neq A} E_{int}^{AB} \tag{18}$$

where

$$E_{net}^A = T^A + V_{ne}^{AA} + V_{ee}^{AA} \tag{19}$$

is the net energy of atom A and

$$E_{int}^{AB} = V_{ne}^{AB} + V_{ne}^{BA} + V_{ee}^{AB} + V_{nn}^{AB} \tag{20}$$

is the total interaction energy between atoms A and B. Each atomic net energy, E_{net}^A, is an effective one-body term that carries all the intra-atomic energy contributions, while each interaction term, E_{int}^{AB}, is an effective two-body component of the total energy. Both contributions actually include all the many-body interactions that result from a quantum-mechanical calculation. However, since the molecular Hamiltonian is expressed as a sum of one- and two-particle terms only, the total energy does not contain explicit many-body interactions.

Equation 18 defines the present energy partition. It states that the total energy can be exactly written as a sum of the net energies of all the atoms of the system and the interatomic interaction energies. It has been derived from the molecular wave function without resorting to the approximations involved in its calculation or to the specific peculiarities of the orbital description used to obtain it. Moreover, the partition is general in the sense that it can be applied with any definition of the atomic densities $\rho^A(\mathbf{r})$, provided that they satisfy eq 1

B. Analysis of the Energy Components. Both E_{net}^A (eq 19) and E_{int}^{AB} (eq 20) can be partitioned into more detailed components with a clear physical meaning. This is possible thanks to the natural decomposition of $\rho_2(\mathbf{r}_1,\mathbf{r}_2)$ in Coulomb and exchange-correlation components:

$$\rho_2(\mathbf{r}_1,\mathbf{r}_2) = \rho_2^C(\mathbf{r}_1,\mathbf{r}_2) + \rho_2^{xc}(\mathbf{r}_1,\mathbf{r}_2) \tag{21}$$

where $\rho_2^C(\mathbf{r}_1,\mathbf{r}_2) = \rho(\mathbf{r}_1)\,\rho(\mathbf{r}_2)$. On the other hand, even though the meaning of exchange and correlation energies is strictly lost as soon as correlated wave functions are used,[28] a reasonable separation of both terms can be performed, defining the exchange density matrix, $\rho_2^X(\mathbf{r}_1,\mathbf{r}_2)$, as in a monodeterminantal case (Fock−Dirac exchange)

$$\rho_2^X(\mathbf{r}_1,\mathbf{r}_2) = -\rho_1(\mathbf{r}_2,\mathbf{r}_1)\,\rho_1(\mathbf{r}_1,\mathbf{r}_2) \tag{22}$$

and the correlation density matrix, $\rho_2^{corr}(\mathbf{r}_1,\mathbf{r}_2)$, by difference

$$\rho_2^{corr}(\mathbf{r}_1,\mathbf{r}_2) = \rho_2 - \rho_2^C - \rho_2^X = \rho_2^{xc} - \rho_2^X \tag{23}$$

Equations 21−23 allow us to write V_{ee}^{AB} as

$$V_{ee}^{AB} = V_C^{AB} + V_{xc}^{AB} \tag{24}$$

$$V_{ee}^{AB} = V_C^{AB} + V_X^{AB} + V_{corr}^{AB} \tag{25}$$

where

$$V_\tau^{AB} = \int\int \frac{\rho_2^{\tau,AB}(\mathbf{r}_1,\mathbf{r}_2)}{r_{12}}\, d\mathbf{r}_1\, d\mathbf{r}_2 \tag{26}$$

$\tau = C$, xc, X, or corr, and

$$\rho_2^{\tau,AB}(\mathbf{r}_1,\mathbf{r}_2) = \rho_2^\tau(\mathbf{r}_1,\mathbf{r}_2)\, w_A(\mathbf{r}_1)\, w_B(\mathbf{r}_2) \tag{27}$$

When eqs 21−23 are used, the intra-atomic repulsion energy V_{ee}^{AA} (eq 16) may also be expressed as a sum of Coulomb, exchange, and correlation contributions:

$$V_{ee}^{AA} = V_C^{AA} + V_{xc}^{AA} \tag{28}$$

$$V_{ee}^{AA} = V_C^{AA} + V_X^{AA} + V_{corr}^{AA} \tag{29}$$

where the expression for V_τ^{AA} is similar to that of V_τ^{AB} (eq 26) but using $^1/_2\rho_2^{AA}$ instead of ρ_2^{AB}.

The atomic net energies (eq 19) contain the same energetic contributions present in the isolated atoms. When the atomic density does not change much for a given atom in different molecules, its energy components (kinetic energies, nuclear attraction to its atomic nucleus, and electron−electron repulsion) will be largely the same. Consequently, the net energies carry the atomic identity from system to system. The deformation energy

$$E_{def}^A = E_{net}^A - E_0^A \tag{30}$$

where E_0^A is the net energy of atom A in vacuo, provides a measurement of the change suffered by an atom in going from the isolated state to the molecule. It plays an important role in the definition of the molecular binding energy, E_{bind}. This property is defined as the total molecular energy referred to an appropriate reference. Taking the isolated neutral atoms' reference, we have

$$E_{\text{bind}} = E - \sum_A E_0^A \tag{31}$$

and using eqs 18 and 30, we obtain

$$E_{\text{bind}} = \sum_A E_{\text{def}}^A + \frac{1}{2}\sum_A \sum_{B\neq A} E_{\text{int}}^{AB} \tag{32}$$

The stability of a molecule with respect to its atomic components is, thus, determined by two factors: the deformation energy, which is necessarily positive in homonuclear diatomic molecules[26] and is usually positive (provided that the neutral atoms are taken as references to define E_{bind}) in many other cases, and the interaction between the atoms, which is usually negative when *A* and *B* are bonded.

When eqs 24 and 25 are used in eq 20, the total interaction energy, E_{int}^{AB}, can be written as

$$E_{\text{int}}^{AB} = V_{\text{cl}}^{AB} + V_{\text{xc}}^{AB} \tag{33}$$

$$E_{\text{int}}^{AB} = V_{\text{cl}}^{AB} + V_X^{AB} + V_{\text{corr}}^{AB} \tag{34}$$

where

$$V_{\text{cl}}^{AB} = V_{\text{ne}}^{AB} + V_{\text{ne}}^{BA} + V_{\text{nn}}^{AB} + V_C^{AB} \tag{35}$$

is the classical electrostatic Coulomb interaction and V_{xc}^{AB} is the interaction energy due to purely quantum effects (i.e., exchange and correlation). This rearrangement is very convenient since the four components of E_{int}^{AB} in eq 20 are usually orders of magnitude larger than the interaction energy itself. However, V_{cl}^{AB}, which can be written in the compact form

$$V_{\text{cl}}^{AB} = \int \frac{\rho_A^T(\mathbf{r}_1)\,\rho_B^T(\mathbf{r}_2)}{r_{12}}\,d\mathbf{r}_1\,d\mathbf{r}_2 \tag{36}$$

where $\rho_A^T(\mathbf{r}) = Z_A\delta(\mathbf{r} - \mathbf{R}_A) - \rho_A(\mathbf{r})$ is the total (nuclear plus electron) charge density of atom *A*, will always be much smaller than each of the individual terms in eq 35.[23] In fact, it can be shown that V_{cl}^{AB} is necessarily positive for two non-interpenetrating and specular distributions of charge. As we will see later, this means that $V_{\text{cl}}^{AB} > 0$ for the two QTAM atoms of a homonuclear diatomic molecule. Since, in these molecules, $E_{\text{def}}^A > 0$, we conclude that the stability of a homonuclear diatomic molecule in the QTAM energy partitioning scheme is a pure quantum phenomenon; that is, it is exclusively due to the interatomic exchange-correlation stabilizing interactions, the rest of energetic components being overall repulsive. We will also see below that this is not necessarily true when overlapping atomic densities $\rho_A(\mathbf{r})$ are used to construct $\rho(\mathbf{r})$.

A measure of the delocalization of electrons of atom *A* in atom *B* and vice versa is given by

$$F_{AB} = 2\int \rho_2^{\text{xc},AB}(\mathbf{r}_1,\mathbf{r}_2)\,d\mathbf{r}_1\,d\mathbf{r}_2 \tag{37}$$

For each *AB* pair, $\delta_{AB} = |F_{AB}|$ is the delocalization index, which can be roughly interpreted as the number of electron bonding pairs shared by the atoms. In this sense, δ_{AB} is a good quantum-mechanical indicator of covalency.

C. Charge Density Partitions. There exists an arbitrary number of ways to partition $\rho(\mathbf{r})$ into atomic densities.[11,26,29,30] One of the methods more firmly rooted in the basic principles of quantum mechanics is the exhaustive partition of $\mathbb{R}^3$ into proper open quantum systems provided by the QTAM of Bader and co-workers.[11,31,32] The theory divides the space into the 3D attraction basins of the gradient field of $\rho(\mathbf{r})$. These atomic basins Ω_A usually contain one and only one nucleus, and they are bounded by a zero local flux surface of $\nabla\rho$ [$\nabla\rho(\mathbf{r})\cdot\mathbf{n}(\mathbf{r}) = 0$ for $\mathbf{r} \in S(\Omega_A)$, where $\mathbf{n}(\mathbf{r})$ is a vector normal to the surface $S(\Omega_A)$]. The QTAM partition can be recast in the form given in eq 1 by simply choosing $w_A(\mathbf{r}) = 1$ for $\mathbf{r} \in \Omega_A$ and $w_A(\mathbf{r}) = 0$ for $\mathbf{r} \notin \Omega_A$.

The QTAM atoms have sharp and well-defined boundaries, present in some cases in irregular forms, and are computationally very costly to determine. Some of these inconveniences can be avoided in the partitions of $\rho(\mathbf{r})$ on the basis of interpenetrating atomic densities (IADs).[26,29,30]

Among the many possibilities, the IADs proposed by Hirshfeld[29] are those preserving as much as possible of the information contained in the charge densities of the isolated atoms.[33] In this partition, each $w_A(\mathbf{r})$ is defined as the ratio of the in vacuo charge density of atom *A* to that of the *promolecule* (set of in vacuo atoms placed at the positions of the nuclei in the actual molecule), that is, $w_A(\mathbf{r}) = \rho_A^0(\mathbf{r})/\sum_A \rho_A^0(\mathbf{r})$. Since the atomic densities of the isolated atoms are required to determine the $w_A(\mathbf{r})$ values, neither an energy partition nor a population analysis can be performed within this scheme based only on the molecular wave function. One is necessarily forced to choose some external atomic densities. To avoid this requirement, we have considered, in this work, the following variation of the Hirshfeld's partition. Taking into account that $\rho(\mathbf{r})$ is usually given in terms of one-center and two-center contributions

$$\rho(\mathbf{r}) = \sum_A \rho_A^0(\mathbf{r}) + \sum_{A\neq B} \rho_{AB}^0(\mathbf{r}) \tag{38}$$

$$\rho_A^0(\mathbf{r}) = \sum_a \sum_{a'} \rho_{aa'}^{AA}\,\phi_a^A(\mathbf{r})\,\phi_{a'}^A(\mathbf{r}) \tag{39}$$

$$\rho_{AB}^0(\mathbf{r}) = \sum_a \sum_b \rho_{ab}^{AB}\,\phi_a^A(\mathbf{r})\,\phi_b^B(\mathbf{r}) \tag{40}$$

where $\phi_a^A(\mathbf{r})$ is a primitive Gaussian function centered at nucleus *A*; we define $w_A(\mathbf{r}) = \tilde{\rho}_A^0(\mathbf{r})/\sum_A \tilde{\rho}_A^0(\mathbf{r})$, where $\tilde{\rho}_A^0(\mathbf{r}) = c_A\,\rho_A^0(\mathbf{r})$ and c_A is a constant chosen such that $\int \tilde{\rho}_A^0(\mathbf{r})\,d\mathbf{r} = Z_A$. Although this partition (Mod-H from now on) is formally equivalent to that of Hirshfeld, it only requires the wave function of the system. We want to remark, at this point, that the modified atomic density $\tilde{\rho}_A^0(\mathbf{r})$ is used

exclusively to define the $w_A(\mathbf{r})$, and they enter the partition into $\rho_A(\mathbf{r})$ only through $w_A(\mathbf{r})$, not through $\rho(\mathbf{r})$ (see eq 1).

Another widely used partition of $\rho(\mathbf{r})$ in terms of IADs is that of Becke,[34] which was initially proposed to simplify the numerical evaluation of monoelectronic multicenter integrals in DFT.[34] It consists of dividing the $\mathbb{R}^3$ space into atomic regions that resemble fuzzy Voronoi polyhedra. The size of each atomic region is adjusted by using an effective radius R_A for each of the atoms of the molecule. In the original work,[34] and also in most of the works that use this partition, R_A is taken as the Bragg−Slater radius of the isolated atom. However, this choice produces very unrealistic atomic charges in many cases. For this reason, we will also use here atomic radii derived from a topological analysis of $\rho(\mathbf{r})$. Provided that a bond critical point (BCP) of $\rho(\mathbf{r})$ exists between atoms A and B, R_A (R_B) is taken as the distance from atom A (B) to the BCP. The number of topological radii of a given atom is, thus, equal to the number of bonds of this atom. In the case that no BCP exists between atoms A and B, R_A is taken as in the original work, that is, as the Bragg−Slater radius of the isolated atom. Becke's partition of $\rho(\mathbf{r})$ based on topological radii is labeled B-Top in this work.

Finally, in the partition method recently developed by Rico et al.,[30] $\rho_A(\mathbf{r})$ is determined following a minimal deformation criterion (MinDef in what follows) for every two-center contribution to $\rho(\mathbf{r})$. Writing each of these contributions as $\rho_{ab}^{AB}\,\phi_a^A(\mathbf{r})\,\phi_b^B(\mathbf{r})$, where ρ_{ab}^{AB} is a density matrix coefficient and $\phi_a^A(\mathbf{r})$ and $\phi_b^B(\mathbf{r})$ are primitive Gaussian functions centered at A and B, respectively (with orbital exponents ζ_A and ζ_B), the MinDef method assigns its entire value to atom A if $\zeta_A > \zeta_B$ or to atom B if $\zeta_B > \zeta_A$. If both orbital exponents are equal, half of each two-center contribution is assigned to each center. In practical terms, the classical Mulliken's partition only differs from the MinDef method in that the former always performs a symmetric partition of each two-center contribution regardless of the values of ζ_A and ζ_B.

D. Computational Aspects. We have shown in ref 25 how, in many of the actual quantum mechanical molecular computations, ρ_2 and ρ_2^X can be written in the forms

$$\rho_2(\mathbf{r}_1,\mathbf{r}_2) = \sum_i^M \lambda_i\, F_i(\mathbf{r}_1)\, F_i(\mathbf{r}_2) \tag{41}$$

$$\rho_2^X(\mathbf{r}_1,\mathbf{r}_2) = \sum_i^M \eta_i\, G_i(\mathbf{r}_1)\, G_i(\mathbf{r}_2) \tag{42}$$

where $M = m(m+1)/2$, m is the number of partially or fully occupied (real) molecular orbitals ϕ_p in the wave function, each $F_i(\mathbf{r})$ and $G_i(\mathbf{r})$ is a known linear combination of products $\phi_p(\mathbf{r})\,\phi_q(\mathbf{r})$, and λ_i and η_i are also known coefficients.

The use of eqs 41 and 42 greatly reduces the computational effort of the two-electron integrations which are necessary to apply our energy partition method. All of these two-electron integrals over arbitrary regions of space can be efficiently computed for both monodeterminantal[24] and correlated[25] wave functions by means of an always-convergent generalization of the conventional multipolar approach (even for overlapping densities). In refs 24 and 25, the procedure was particularized to the QTAM atomic basins. However, the method can be applied as well to general tridimensional regions. In particular, it can be used with the fuzzy-boundary regions defined in the previous two subsections. The required computational effort can also be substantially reduced by computing and storing for further use the radial factors

$$R_{lm}^{\Omega_A}(r) = \left(\frac{4\pi}{2l+1}\right)^{1/2} \int_{\hat{r}} S_{lm}(\hat{r})\, f^{\Omega_A}(\mathbf{r})\, \mathrm{d}\hat{r} \tag{43}$$

for all the grid points of an appropriate radial quadrature. In eq 43, $\hat{r} = (\theta,\phi)$; $S_{lm}(\hat{r})$ is a real spherical harmonic, defined as in ref 24; and $f^{\Omega_A}(\mathbf{r})$ is $\rho_A(\mathbf{r})$, $F_i^A(\mathbf{r}) = w_A(\mathbf{r})\,F_i(\mathbf{r})$, or $G_i^A(\mathbf{r}) = w_A(\mathbf{r})\,G_i(\mathbf{r})$, where $F_i(\mathbf{r})$ [$G_i(\mathbf{r})$] is one the functions of eq 41 (eq 42). Let us recall that the bipolar expansion for r_{12}^{-1} used in this work is always convergent.[24] Nevertheless, simpler integration methods based on a standard multipolar expansion of r_{12}^{-1}, used for instance by Popelier et al.,[35−37] converge to the exact results for sufficiently separated atoms. In this standard multipolar approach, the Coulombic interaction between $\rho_A(\mathbf{r}_1)$ and $\rho_B(\mathbf{r}_2)$ is given by[24]

$$V_{\mathrm{C,lr}}^{AB} = \sum_{l_1m_1l_2m_2}^{\infty}\sum^{\infty} C_{l_1m_1l_2m_2} \frac{Q_{l_1m_1}^{\Omega_A} Q_{l_2m_2}^{\Omega_B}}{R^{l_1+l_2+1}} \tag{44}$$

where $C_{l_1m_1l_2m_2}$ is a coupling coefficient[24] and $Q_{lm}^{\Omega_A}$ are spherical atomic multipoles defined as

$$Q_{lm}^{\Omega A} = \left(\frac{4\pi}{2l+1}\right)^{1/2} \int r^l\, S_{lm}(\hat{r})\, \rho_A(\mathbf{r})\, \mathrm{d}\mathbf{r} \tag{45}$$

The differences between the approximate and exact multipoles or between V_{C}^{AB} (eq 26, exact) and $V_{\mathrm{C,lr}}^{AB}$ (eq 44, approximate) will indicate how strongly atoms A and B overlap.

III. Results and Discussion

In this section, we present the results of our energy partition method. First, we analyze the atomic densities and charges of both atoms of CO and comment on the results obtained in some other molecules (Subsection IIIA). In Subsection IIIB, we give a thorough analysis of the dihydrogen molecule, a paradigm in which any new idea or method should be tested on. Finally, the N_2 and LiH molecules, which may be considered representative of the covalent (N_2) and ionic (LiH) bonding types, will be analyzed.

All the calculations have used the *gamess* code[38] to obtain the wave functions and our *promolden* code to perform the energy partition. The wave functions have been computed in the ground electronic states using complete active space CAS[n,m] (n active electrons, m active orbitals) multiconfiguration calculations for H_2 ($CAS^{2,2}$), N_2 ($CAS^{10,10}$), and LiH ($CAS^{2,2}$) and a Hartree−Fock (HF) calculation for CO. Basis sets 6-311G(p), TZV(d), 6-311G(p), and TZV(2p,-3d)++ were used for H_2, N_2, LiH, and CO, respectively. The energy components in *promolden* have been computed to an accuracy of about 1.0−3.0 kcal/mol.

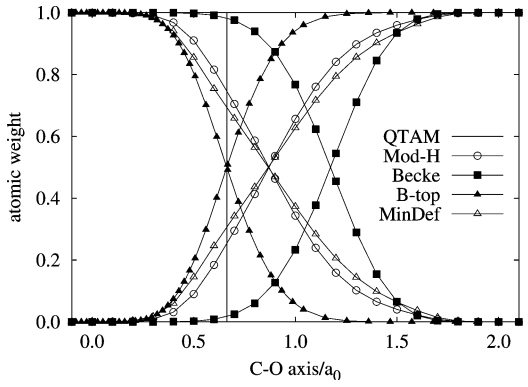

Figure 1. HF/TZV(2p,3d)++ atomic functions $w_A(\mathbf{r})$ for the carbon and oxygen atoms in the CO molecule along the internuclear axis. The C and O atoms are at the −0.0424 and 2.0424 positions along the C−O axis, respectively. Labels Becke, B-Top, MinDef, and Mod-H stand for the Becke with Bragg−Slater radii, Becke with topological radii, Rico et al. minimal deformation criterion, and modified Hirshfeld methods, respectively.

A. Atomic Overlapping Densities and Charges. The differences and similarities between the various partitions of $\rho(\mathbf{r})$ can be appreciated in Figure 1, where we have plotted $w_A(\mathbf{r})$ for both atoms in the CO molecule along the internuclear axis. In this figure, the QTAM $w_A(\mathbf{r})$ function is given by a vertical line at the BCP ($r_C = 0.705\ a_0$ and $r_O = 1.380\ a_0$). All the partitions generate localized atomic densities, and they basically differ in the size extension assigned to each atom. For a diatomic molecule, it is easy to show that, in the Becke and B-Top partitions, the point where $w_A = w_B = {}^1/_2$ along the $A-B$ axis satisfies $r_A/r_B = R_A/R_B$ [at this point $\rho_A(\mathbf{r}) = \rho_B(\mathbf{r}) = \rho(\mathbf{r})/2$, i.e., half of the charge density is assigned to atom A and half to atom B]. Consequently, when the Slater−Bragg radii of the isolated C and O atoms are used (0.65 a_0 and 0.47 a_0, respectively), this point is much closer to the oxygen atom ($r_O = 0.875\ a_0$) than to the carbon atom ($r_C = 1.210\ a_0$). However, when topological radii ($R_C^{top} = 0.705\ a_0$ and $R_O^{top} = 1.380\ a_0$) are used instead, that point moves to the BCP of the molecule. These numbers show that, in going from C to O along the C−O axis, $w_C(\mathbf{r})$ decays to zero much earlier in the B-Top than in the Becke partition, which means that a great quantity of electronic charge, ascribed to C in the Becke partition scheme, actually belongs to O in the B-Top method. This produces a change in the charge-transfer direction of the C−O bond in both cases ($C^{\delta-}O^{\delta+}$ in the Becke partition versus $C^{\delta+}O^{\delta-}$ in the B-Top partition).

In heterodiatomic molecules, the points in $\mathbb{R}^3$ for which $w_A = w_B = {}^1/_2$ in the B-Top partition do not necessarily lie on the QTAM interatomic surface. Of course, the BCP, which lies on this surface, is a notable exception since it satisfies the above property. Consequently, we expect that out of, but not very far from, the internuclear axis, the points in $\mathbb{R}^3$ for which $w_A = w_B = {}^1/_2$ will probably be relatively close to the QTAM interatomic surface. This explains the similarities between QTAM and B-Top atomic charges that we have found in many molecules. Of course, for homonuclear diatomic molecules, the points where $w_A = w_B = {}^1/_2$ always lie on the QTAM interatomic surface. Since, in the limit $k \to \infty$ (where k is the characteristic iterative parameter in the Becke partition method, see ref 34), $w_A(\mathbf{r})$ transforms to a steplike function [$w_A(\mathbf{r}) = 1$ for $r_A \le r_B$ and $w_A(\mathbf{r}) = 0$ for $r_A > r_B$], the QTAM and B-Top atoms, and all their properties and intra-atomic and interatomic interactions, tend to be equal as k increases in homonuclear diatomic molecules. This need not be so in heterodiatomics.

Table 1. HF/TZV(2p,3d)++ Atomic Charges for the Carbon and Oxygen Atoms of the CO Molecule from Different Partition Methods of $\rho(\mathbf{r})$[a]

	M	H	B	QTAM	Mod-H	B-Top	MinDef
C	0.448	0.124	−0.406	1.353	0.497	1.204	0.303
O	−0.448	−0.124	0.406	−1.356	−0.497	−1.204	−0.303

[a] M, H, and B letters stand for Mulliken, Hirshfeld, and Becke partitions, respectively. Labels B-Top, MinDef, Mod-H, and QTAM have been defined in the text.

The atomic charges derived by integrating $\rho_A(\mathbf{r})$ for the carbon and oxygen atoms of the CO molecule using the Becke, B-Top, MinDef, Mod-H, and QTAM partitions, as well as those obtained from the classical Mulliken and the original Hirshfeld partitions, are collected in Table 1. The Hirshfeld $w_A(\mathbf{r})$ functions were computed from the high-quality Koga's atomic densities of the isolated carbon and oxygen atoms.[39] The charge transfer (CT) predicted by the Becke partition ($C^{\delta-}O^{\delta+}$) is contrary to that obtained in all the other methods ($C^{\delta+}O^{\delta-}$). Analyzing the atomic charges obtained for many other molecules, we have observed that this partition behaves generally very differently from the rest, predicting, in many cases, a charge transfer that is even contrary to traditional chemical thinking. When a molecule is formed from neutral atoms, the effective atomic radii change with respect to their in vacuo values, this change increasing with the difference of electronegativities of both atoms. It seems that Becke's method does not properly account either for this changeor for the actual charge-transfer phenomena in the molecule.

The deficiencies of Becke's atomic charges can be minimized by computing $w_A(\mathbf{r})$ from topological atomic radii. The B-Top method gives atomic charges which are much more reasonable from a chemical point of view and which are fairly similar to those derived from the QTAM. Both the B-Top and QTAM charges suggest a relatively high charge transfer in the CO molecule. This behavior is general and also happens in many other molecules. On the other hand, Mod-H and MinDef schemes give atomic charges fairly close to each other and offer, in general, an image with more neutral atoms than B-Top and QTAM partitions. The Hirshfeld method provides the more neutral atoms in most cases. This fact is well-known and has been previously observed in a large variety of molecules (see ref 40 and references therein). It is noteworthy that, since the atomic functions $w_A(\mathbf{r})$ in the Becke and Hirshfeld schemes are completely independent of the details of the molecular wave functions, they produce atomic charges which are practically basis-set-independent. This feature of the Hirshfeld atomic charges was also observed in ref 40. We do not think this fact implies that they are more realistic than those of other partitions. It is simply a characteristic feature of these two

methods that, obviously, would also be desirable in all of the other cases, thus making the discussion of results easier and avoiding the inconveniences derived from the change of these results with the basis set employed in the calculation.

The total molecular dipole (μ) of a neutral molecule is given (in atomic units) by[11]

$$\mu = \sum_A Z_A \mathbf{R}_A - \int \mathbf{r}\rho(\mathbf{r})\, d\mathbf{r} \qquad (46)$$

where the electronic and nuclear position vectors $\mathbf{r}$ and $\mathbf{R}_A$ are measured from a common, arbitrary origin. Using $\mathbf{r}_A = \mathbf{r} - \mathbf{R}_A$, where $\mathbf{r}_A$ is the electronic position vector with respect to nucleus A, one can transform μ to give

$$\mu = \sum_A Q_A \mathbf{R}_A - \sum_A \int \mathbf{r}_A\, \rho_A(\mathbf{r})\, d\mathbf{r} = \mu_c + \mu_a \qquad (47)$$

where Q_A is the total (nuclear plus electronic) charge of atom A. The first term in eq 47, μ_c, is the contribution from the interatomic charge transfer, while the second, μ_a, arises from the polarization of the individual atomic distributions. Both are important in determining μ, although μ_c usually dominates when there is a significant charge transfer. In diatomic molecules, the polarity of μ_c can be generally inferred from the electronegativities of both atoms. In the CO molecule, it must be clearly of the form $C^{\delta+}O^{\delta-}$, which is the one exhibited in Table 1 by all except the Becke partition. This result does not contradict the fact that total polarity in CO is the opposite (i.e., $C^{\delta-}O^{\delta+}$, as is now the consensus from high-level calculations, and happens also in our HF calculation) since the polarization contribution (μ_a), in this case, opposes and dominates μ_c.

B. Energy Partition in H_2. The first example in which we analyze the energy partition is H_2 in the $^1\Sigma_g^+$ ground state at the CAS[2,2]/6-311G(p) level of calculation. Since the QTAM results have been discussed in detail elsewhere,[23] we will concentrate here on the comparison of these results with those obtained in the other partitions. Moreover, since H_2 is homonuclear, Becke and B-Top partitions are, in this case, equivalent. The relative values of the energy components can be rationalized in terms of the shapes of their atomic densities $\rho_A(\mathbf{r})$ and weights $w_A(\mathbf{r})$. We have depicted $\rho_A(\mathbf{r})$ for the left hydrogen of H_2 (left-H) along the internuclear axis in Figure 2. As expected, all densities are very close to each other to the left of the nucleus, differing only in the right region: the rate of decay of $\rho_A(\mathbf{r})$ is QTAM > B-Top > Mod-H > MinDef. Obviously, from the equation $\rho_A(\mathbf{r}) = \rho(\mathbf{r})\, w_A(\mathbf{r})$, the same can be said of the $w_A(\mathbf{r})$'s. The right tail of $\rho_A(\mathbf{r})$ in Figure 2 for the B-Top, Mod-H, and MinDef partitions shows a shift of QTAM electron charge from the left-H region to the right of the normal plane bisecting the H−H internuclear axis, increasing the interpenetration of the two atomic densities in the order QTAM < B-Top < Mod-H < MinDef. The charge redistribution from the neighborhood of the left-H should decrease the magnitude of V_{ne}^{AA}, directly dependent on $\rho_A(\mathbf{r})$. In the same way, the more concentrated the left-H $\rho_A(\mathbf{r})$ is on its own nucleus, the greater the value of V_C^{AA} will be. According to these arguments, the magnitudes of V_{ne}^{AA} and V_C^{AA} should decrease in the order QTAM > B-Top > Mod-H > MinDef. On the other hand, V_τ^{AA} (τ = xc, X, corr) values are given by eq 26 (halved and with $A = B$) with $\rho_2^{\tau,AA}(\mathbf{r}_1,\mathbf{r}_2) = w_A(\mathbf{r})^2\, \rho_2(\mathbf{r}_1,\mathbf{r}_2)$. From our previous discussion on the behavior of the $w_A(\mathbf{r})$'s in the different partitions, we expect that the magnitudes of these three energy components (all of them negative) also decrease in the above order.

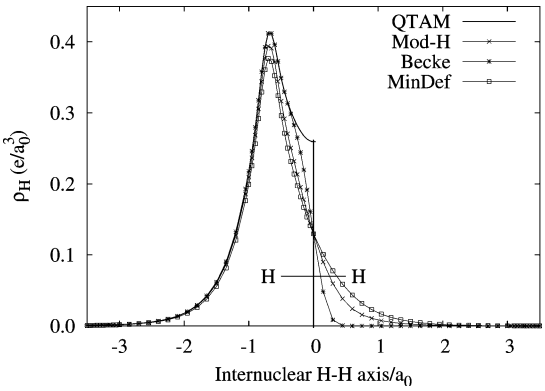

Figure 2. CAS[2,2]/6-311G(p) atomic density for the left atom of H_2 along the internuclear axis. Left and right hydrogens are at −0.7 and +0.7 a_0, respectively. Labels Becke, MinDef, Mod-H, and QTAM have been defined in the text.

The energy components at the experimental geometry (R_{exp} = 0.7414 Å) are collected in Table 2 and fully confirm the above predictions. The last row in this table collects the binding energy computed by using eq 32. In the four cases, it differs from the analytical value (eq 31) by less than 0.2 mhartree. This number may, thus, be taken as an estimate of the numerical error in the integrations.

Let us now focus on the intra-atomic properties in Table 2 (first block). As we can see, the atomic kinetic energy T^A is the same in the four partitions. Although this property suffers (except in the QTAM decomposition scheme) from the nonuniqueness of the kinetic energy density, the total molecular kinetic energy density ($\hat{T}$) is well-defined in all the schemes. Consequently, in homonuclear diatomic molecules, where both atoms are equivalent by symmetry, T^A is necessarily equal to half the total kinetic energy.

Since V_{ee}^{AA} (see eq 28) is dominated by the Coulomb part, its magnitude shows the same trend as V_C^{AA}, decreasing in the order QTAM > B-Top > Mod-H > MinDef. Nevertheless, the differences between the V_{ee}^{AA} values in the different partitions are an order or magnitude smaller than those obtained for the V_{ne}^{AA}. Since T^A is the same in all the partitions because of symmetry reasons, we conclude that V_{ne}^{AA} is the main factor determining the differences between the net energies in the different partitions.

The final intra-atomic balance gives E_{def}^A values that increase according to the sequence QTAM < B-Top < Mod-H < MinDef. This quantity is necessarily positive in homonuclear diatomic molecules,[26] so the hydrogen atom in H_2 is less destabilized with respect to the isolated state in the QTAM than in the other three partitions. In this sense, the QTAM partition is the one best preserving the atomic identity upon molecule formation. Although we have not carried out Li and Parr's division of $\rho(\mathbf{r})$, which explicitly minimizes the deformation energy,[26] it would give an E_{def}^A

Table 2. CAS[2,2]/6-311G(p) Energy Components (hartree) for H_2 at the Experimental Geometry from Different Partition Methods of $\rho(\mathbf{r})$[a]

property	QTAM	Mod-H	Becke	MinDef
T^A	0.5805	0.5805	0.5805	0.5805
V_{ne}^{AA}	−1.2278	−1.1545	−1.2149	−1.1150
V_{ee}^{AA}	0.1628	0.1590	0.1614	0.1581
V_{xc}^{AA}	−0.2367	−0.2083	−0.2299	−0.1968
V_C^{AA}	0.3995	0.3673	0.3913	0.3549
V_X^{AA}	−0.1988	−0.1818	−0.1945	−0.1753
V_{corr}^{AA}	−0.0378	−0.0265	−0.0354	−0.0216
ΔT^A	0.0807	0.0807	0.0807	0.0807
ΔV_{ne}^A	−0.2282	−0.1549	−0.2153	−0.1154
ΔV_{ee}^A	0.1628	0.1590	0.1614	0.1581
E_{net}^A	−0.4844	−0.4150	−0.4730	−0.3764
E_{def}^A	0.0154	0.0848	0.0268	0.1234
V_{ne}^{AB}	−0.5976	−0.6708	−0.6104	−0.7104
V_{ee}^{AB}	0.2994	0.3069	0.3021	0.3088
V_{cl}^{AB}	0.0423	−0.0398	0.0329	−0.0942
V_{xc}^{AB}	−0.2244	−0.2811	−0.2379	−0.3040
δ_{AB}	0.8334	0.9082	0.8502	0.9406
V_C^{AB}	0.5238	0.5880	0.5399	0.6127
V_X^{AB}	−0.2523	−0.2863	−0.2608	−0.2993
V_{corr}^{AB}	0.0279	0.0052	0.0230	−0.0046
E_{int}^{AB}	−0.1821	−0.3209	−0.2050	−0.3982
E_{bind}[b]	−0.1514	−0.1514	−0.1513	−0.1514

[a] $\Delta X^A = X^A(H_2) - X^A(H_{vac})$. Labels Becke, MinDef, Mod-H, and QTAM have been defined in the text. [b] The analytical value computed with eq 31 from the total atomic and molecular energies given by the gamess code is −0.1515 hartree.

value smaller than that of the QTAM partition. However, since our results in Table 2 nicely correlate with the general aspect of $\rho_A(\mathbf{r})$ in Figure 2, Li and Parr's $\rho_A(\mathbf{r})$ will probably be very localized on its own nucleus as the QTAM $\rho_A(\mathbf{r})$. It is also interesting to remark that, as Nalewajski et al. have recently shown,[41−43] the best transferability of the atoms from the isolated state to the molecule in the information theoretical sense is obtained when $\rho(\mathbf{r})$ is given in terms of Hirshfeld atomic densities. Preliminary results using our energy decomposition scheme fed with Hirshfeld atoms have shown, however, that, in an energetic sense, they are rather similar to the Mod-H and MinDef atoms and considerably less transferable than QTAM atoms.

We analyze now the interatomic energy components (second block in Table 2). Since each total interaction term (V_{ne}, V_C, V_{xc}, V_X, ...) is clearly independent of the partition used for $\rho(\mathbf{r})$, each of the interatomic stabilizing contributions (V_{ne}^{AB}, V_{xc}^{AB}, and V_X^{AB}) decreases now in the order MinDef < Mod-H < B-Top < QTAM, which is the opposite of what we obtained for the corresponding intra-atomic terms.

It is interesting to remark that, contrary to the intra-atomic correlation energy (V_{corr}^{AA}), which plays a stabilizing role, the interatomic correlation (V_{corr}^{AB}) destabilizes the H_2 molecule (except in the MinDef partition). The interatomic electron−electron repulsion is very similar in the four partitions, the largest difference being 5.9 kcal/mol between the QTAM and MinDef partitions. This means that, as in the intra-atomic case, the differences between the four partitions are mainly due to the electrons−nucleus interaction. In the interatomic case, V_{ne}^{AB} is, thus, the main factor causing the considerable increase (in absolute value) of the interaction energy, E_{int}^{AB}, in the order QTAM < B-Top < Mod-H < MinDef.

As shown in eq 33, E_{int}^{AB} can be decomposed in a classical (V_{cl}^{AB}) and a quantum-mechanical interaction (V_{xc}^{AB}). In most energy decomposition methods (see, for instance, ref 16), V_{cl}^{AB} is identified with the classical electrostatic interaction between the two fragments of the molecule. Since the fragment electron densities usually interpenetrate considerably, this is a highly stabilizing interaction on the order of tens or hundreds of kilocalories per mole. As we can see in Table 2, the Mod-H and MinDef partitions, based on *interpenetrating* atoms, give a negative V_{cl}^{AB} value. However, in the B-Top and QTAM partitions, V_{cl}^{AB} is a positive number. There is nothing contradictory in these results since it is trivial to show, using elementary electrostatics, that the classical interaction energy between two strictly nonoverlapping and neutral distributions of charge, one the specular image of the other, is positive. The QTAM atoms in homonuclear diatomics exactly satisfy this condition and, thus, give $V_{cl}^{AB} > 0$. However, V_{cl}^{AB} decreases as the overlap between both atomic densities increases, eventually becoming negative. The B-Top partition is one in which this overlap is not yet so strong as to give a stabilizing electrostatic interaction energy.

The above arguments lead to the following conclusions concerning the QTAM partition. Since, in homonuclear diatomics, $V_{cl}^{AB} > 0$ and $E_{def}^A > 0$, as a result of the absence of charge transfer between both atoms, the interatomic exchange-correlation term V_{xc}^{AB} is the only driving force of binding. As the interatomic overlap increases, V_{cl}^{AB} and V_{xc}^{AB} become more stabilizing, and the binding in H_2 results from a balance between E_{int}^{AB} and E_{def}^A, both quantities greater in absolute value than in the QTAM partition. The delocalization indices δ_{AB} in Table 2 increase in the order δ_{AB}(QTAM) < δ_{AB}(B-Top) < δ_{AB}(Mod-H) < δ_{AB}(MinDef). However, their values are slightly smaller than 1.0 in all the cases, which is typical of a single covalent bond. Notice that δ_{AB} is proportional to the absolute value of the corresponding interatomic exchange-correlation interaction V_{xc}^{AB}. Our results (HF and correlated) in many molecules have shown that this fact is of general validity, so the pure quantum mechanical interaction energy is a good chemical indicator of electron delocalization and of covalency. Moreover, partitioning methods of $\rho(\mathbf{r})$ based on interpenetrating atomic densities tend to give covalency indices higher than those of the QTAM partition.

Several energetic contributions to E_{bind}^A have been plotted in Figure 3 for a wide range of internuclear H−H distances. Looking at the E_{def}^A versus R_{H-H} curves, we observe that E_{def}^A is positive in all the partitions, so the interaction of both atoms has a net energy penalty, as expected. In the QTAM and B-Top partitions, E_{def}^A has a very shallow maximum near 2.5 a_0, runs through a minimum very near the equilibrium geometry, and rises very steeply when we

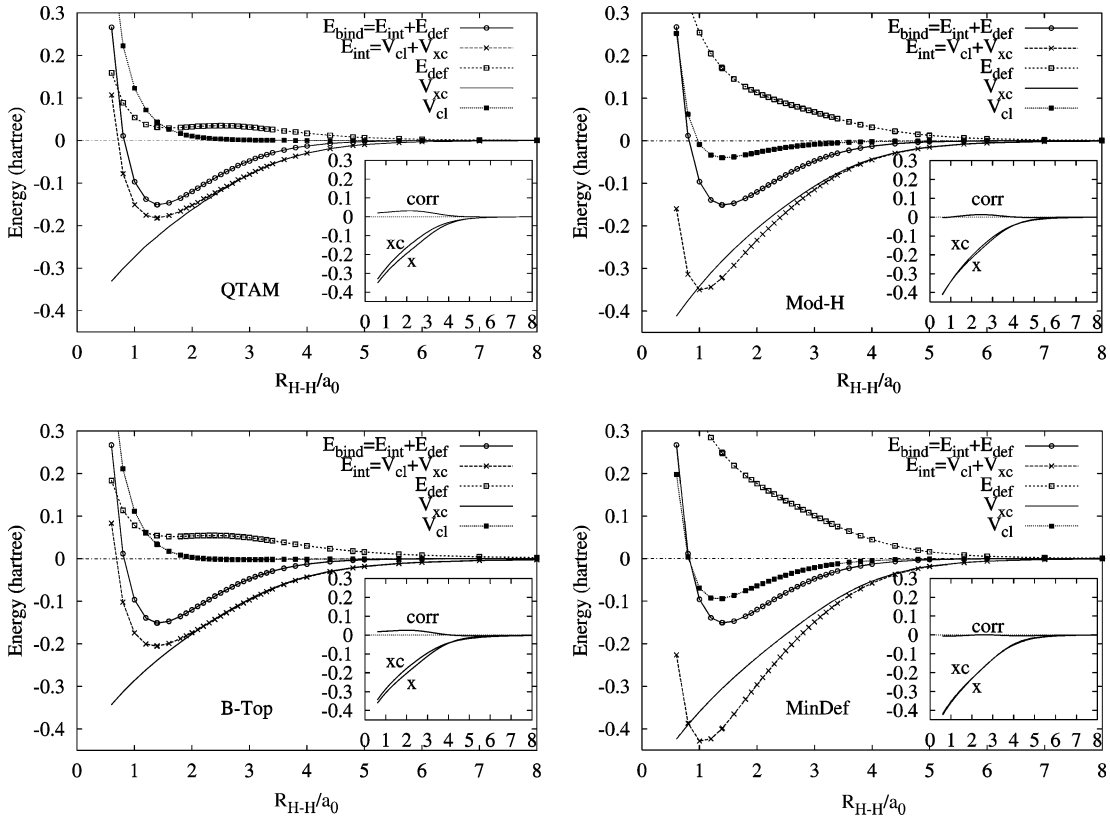

Figure 3. CAS[2,2]/6-311G(p) energy components for H_2 as a function of the internuclear distance. MinDef and Mod-H are the results using the Rico et al. and the modified Hirshfeld partitioning schemes, respectively. The insets show the splitting of V_{xc} into exchange (x) and correlation (corr) contributions.

compress the molecule in excess. However, in the Mod-H and MinDef partitions, E^A_{def} increases continuously when both atoms approach each other. Moreover, E^A_{def} at the equilibrium geometry is very small in the QTAM and B-Top partitions [9.7 (QTAM) and 16.8 (B-Top) kcal/mol]. These numbers should be compared with the corresponding E^A_{net} values [−304.0 (QTAM) and −296.8 (B-Top) kcal/mol]. There is, thus, a clear difference between the QTAM/B-Top and Mod-H/MinDef hydrogen atoms: While QTAM and B-Top hydrogen atoms in the H_2 molecule have almost the same energy that they have in vacuo, Mod-H and MinDef hydrogen atoms in the H_2 molecule are highly destabilized with respect to the isolated state. As a consequence, QTAM and B-Top binding energy curves follow faithfully those of the interaction; that is, a slight increase in deformation energy is traded for a large interaction energy.

Even more interesting is the fact that, from infinity to almost the equilibrium geometry, the interaction energy in the QTAM and B-Top partitions is practically dominated by the pure quantum mechanical interaction V^{AB}_{xc}, the classical interaction V^{AB}_{cl} being almost negligible in that regime of R_{H-H} distances. As we can see in Figure 3, the overall picture in the Mod-H and MinDef partitions is rather different. In these two cases, the binding energy curve results from the sum of two strongly attractive curves (V^{AB}_{xc} and V^{AB}_{cl}) and a strongly repulsive one (E^A_{def}). It is interesting to remark, however, that in all the cases the intercenter exchange-correlation energy, V^{AB}_{xc}, is dominated by the exchange part, which we have to understand here in the sense of Heitler−London resonance energy, and that the intercenter correlation energy, V^{AB}_{corr}, is rather small (almost negligible in the Mod-H and MinDef partitions). Besides this, V^{AB}_{corr} at the equilibrium geometry is a destabilizing contribution in all but the MinDef partition.

C. Energy Partition in N_2. We analyze in this subsection the results of our energy partition methods in the N_2 molecule. The more significant energy components for N_2 at the theoretical equilibrium geometry are gathered in Table 3 (as in H_2, the Becke and B-Top partitions are equivalent). This molecule, as any homonuclear diatomic, lacks electron charge transfer between the atoms. Each of the intra-atomic energy contributions refers, then, to the same number of electrons that a nitrogen atom has in vacuo and can, thus, be compared with its corresponding isolated value. The numbers in Table 3 give us a picture that seems to be a scaled counterpart of that of the H_2 molecule. In N_2, however, the overall numerical error in the integration is considerably larger than in H_2. Here, the binding energy computed through eq 32 is 0.4 (QTAM), 4.3 (Mod-H), 3.6 (B-Top), and 4.5 (MinDef) mhartree larger than the analytical value obtained through eq 31. In the Mod-H, B-Top, and MinDef partitions, this error is necessarily associated with the nuclear attraction and electron repulsion energies since the total kinetic energy in these schemes ($T = 2T^A = 109.1352$ hartree) reproduces with four decimal figures the exact *gamess* value ($T_{analytical} = 109.135\,238$ hartree).

As in that molecule, the different behavior of the four energy partitions in N_2 can also be understood in terms of

Table 3. CAS[10,10]/TZV(d) Energy Components (hartree) for N_2 at the Theoretical Equilibrium Geometry from Different Partition Methods of $\rho(\mathbf{r})$

property	QTAM	Mod-H	B-Top	MinDef
T^A	54.5673	54.5676	54.5676	54.5676
V_{ne}^{AA}	−129.6517	−128.9735	−129.3203	−128.7652
V_{ee}^{AA}	20.7465	20.4185	20.5689	20.3293
V_{xc}^{AA}	−6.3427	−6.2174	−6.2701	−6.1876
V_{C}^{AA}	27.0892	26.6359	26.8390	26.5169
V_{X}^{AA}	−6.0927	−6.0019	−6.0422	−5.9823
V_{corr}^{AA}	−0.2501	−0.2155	−0.2279	−0.2053
E_{net}^{A}	−54.3379	−53.9873	−54.1838	−53.8682
E_{def}^{A}	0.0609	0.4114	0.2149	0.5305
V_{ne}^{AB}	−21.9580	−22.6375	−22.2906	−22.8458
V_{ee}^{AB}	20.0432	20.7051	20.4036	20.8837
V_{cl}^{AB}	0.2216	−0.2253	0.0627	−0.4039
V_{xc}^{AB}	−0.6730	−0.9232	−0.8190	−0.9827
δ_{AB}	1.9395	2.2929	2.1583	2.3729
V_{C}^{AB}	20.7163	21.6284	21.2226	21.8664
E_{int}^{AB}	−0.4514	−1.1485	−0.7563	−1.3866
E_{bind}[a]	−0.3297	−0.3258	−0.3265	−0.3256

[a] The analytical value computed with eq 31 from the total atomic and molecular energies given by the gamess code is −0.3301 hartree.

the form exhibited by the atomic densities of both nitrogen atoms. The interpenetration of these densities increases in the order QTAM < B-Top < Mod-H < MinDef. Correspondingly, the absolute values of all the intra-atomic energy components increase in the opposite sense. The atomic deformation energy, E_{def}^{A}, in the QTAM partition is about 38 kcal/mol. This is a small number and amounts to only 0.11 of the net atomic energy. However, the Mod-H and MinDef partitions give unreasonable deformation energies (258 and 333 kcal/mol, respectively). Again, the B-Top partition, with a deformation energy equal to 135 kcal/mol, gives an intermediate result. From these numbers, it seems that one can only recognize the nitrogen atom in the QTAM partition.

As in H_2, B-Top atomic densities do not interpenetrate sufficiently as to give a negative V_{cl}^{AB} value. However, Mod-H and MinDef partitions give a strongly stabilizing classical interaction. In this sense, they are similar to other energy partition methods based on interpenetrating fragments.[16] Furthermore, the classical interaction energy, except in the B-Top partition, is not a small contribution to the total interaction energy, E_{int}^{AB}. This result contrasts with that observed in H_2, where most of the interaction was due to the exchange-correlation term, V_{xc}^{AB}.

The energy partition in N_2 has been performed in a range of N−N internuclear distances going from 1.2 to 3.6 a_0. Most of the comments concerning H_2 are also pertinent in N_2, and we have, thus, omitted the figure for brevity. From 1.8 up to 3.6 a_0, the atomic deformation energy is practically flat in the QTAM partition, whereas it continuously increases as R_{N-N} decreases in the other partitions, particularly in the Mod-H and MinDef partitions. The absolute value of the classical interaction, V_{cl}^{AB}, is always repulsive (attractive) and decreases with R_{N-N} in the QTAM (Mod-H and MinDef) partition(s). In the B-Top partition, its behavior is very similar to that found in the QTAM partition, although V_{cl}^{AB} becomes slightly attractive for R_{N-N} distances larger than 2.4 a_0. Similarly, the total interaction energy, E_{int}^{AB}, displays a minimum in the QTAM and B-Top partitions while it decreases abruptly and monotonically in the Mod-H and MinDef partitions when R_{N-N} decreases. Moreover, at R_{N-N} distances close to the equilibrium, the E_{int}^{AB} and E_{bind}^{AB} curves do not differ too much in the QTAM partition, whereas they differ greatly in the Mod-H and MinDef partitions.

In summary, we have found that, as in H_2, the QTAM partition is again the one best preserving the atomic identity in passing from the isolated atom to the molecule, followed by the B-Top, Mod-H, and MinDef partitions. Binding in the Mod-H and MinDef partitions arises, thus, as a consequence of a very delicate interplay of large (effective intra-atomic and interatomic) magnitudes, whereas in the B-Top and (more notably) QTAM partitions, it results from an interaction energy slightly contaminated by the intra-atomic destabilizing deformation energy term. Preliminary results in other homonuclear diatomics indicate that this general conclusion is valid as well.

D. Energy Partition in LiH. Let us turn to the LiH molecule. Its more relevant results at the experimental geometry are collected in Table 4. The error in the numerical integrations within the Mod-H, B-Top, and MinDef partitions is rather small (∼0.0−0.1 mhartree), while it is considerably larger in the QTAM partition (∼1.1 mhartree). The total kinetic energy (T) is 8.0119, 8.0118, 8.0118, and 8.0118 hartree in the QTAM, B-Top, Mod-H, and MinDef partitions, respectively. These numbers agree very well with the exact value (8.011874 hartree). It should be stressed, however, that T is shared between the Li and H atoms rather differently in the four schemes. For instance, T^H (QTAM) = 0.6405 hartree, while T^H takes the values 0.6249, 0.5482, and 0.7362 hartree in the B-Top, Mod-H, and MinDef partitions, respectively. Given the good agreement between T (QTAM) and the exact T value, it is clear that, in the QTAM partition, the 1.1 mhartree error in E_{bind} is due to numerical errors in the integration of the nuclear attraction and electron repulsion energies, as it happened in the N_2 molecule within the B-Top, Mod-H, and MinDef schemes.

The QTAM partition predicts that LiH is highly ionic, with atomic charges close to nominal ones. On the contrary, in the Mod-H partition, this molecule presents a relatively low ionicity, while the B-Top and MinDef partitions give intermediate results.

The rationalization of the deformation energy is not as easy as in homonuclear diatomics as a result of the electron density transfer from Li to H. Nevertheless, it is still possible to do some qualitative reasoning about its value and behavior. If the total charge of an atom would remain unchanged when it enters into a molecule, E_{def}^{A} would be strictly positive because of the variational principle. However, in heterodiatomics, one must take into account the change in E_{def}^{A} due to the CT prior to considering the term coming from the exclusive deformation of the density. In LiH, the Li atom loses a fraction (f) of an electron (different depending on

Table 4. CAS[2,2]//6-311G(p) Energy Components for LiH at the Experimental Geometry from Different Partition Methods of $\rho(\mathbf{r})$[a]

properties	QTAM	Mod-H	B-Top	MinDef
Q^{Li}	0.8912	0.4067	0.7076	0.6768
ΔT^{Li}	−0.0608	0.0314	−0.0453	−0.1566
ΔV_{ee}^{LiLi}	−0.4756	−0.1648	−0.3449	−0.3754
ΔV_{ne}^{LiLi}	0.7248	0.3036	0.5450	0.6508
V_{xc}^{LiLi}	−1.6632	−1.6865	−1.6653	−1.6314
V_{X}^{LiLi}	−1.6626	−1.6805	−1.6624	−1.6293
V_{corr}^{LiLi}	−0.0006	−0.0060	−0.0029	−0.0021
E_{def}^{Li}	0.1883	0.1702	0.1548	0.1187
Q^{H}	−0.8907	−0.4062	−0.7074	−0.6763
ΔT^{H}	0.1407	0.0484	0.1251	0.2364
ΔV_{ee}^{HH}	0.4054	0.2598	0.3532	0.3459
ΔV_{ne}^{HH}	−0.5255	−0.3241	−0.4642	−0.4224
V_{xc}^{HH}	−0.4671	−0.3232	−0.4146	−0.3808
V_{X}^{HH}	−0.4231	−0.2825	−0.3713	−0.3406
V_{corr}^{HH}	−0.0440	−0.0407	−0.0433	−0.0401
E_{def}^{H}	0.0205	−0.0159	0.0141	0.1599
V_{ne}^{LiH}	−1.8056	−1.3846	−1.6261	−1.7317
V_{ne}^{HLi}	−0.7006	−1.3846	−0.7620	−1.7317
V_{ee}^{LiH}	1.2285	1.0623	1.1493	1.1868
V_{cl}^{LiH}	−0.2394	−0.0651	−0.1499	−0.1919
$Q^{Li}Q^{H}/R_{Li-H}$	−0.2673	−0.0551	−0.1669	−0.1526
V_{xc}^{LiH}	−0.0383	−0.1591	−0.0889	−0.1567
V_{X}^{LiH}	−0.0377	−0.1605	−0.0897	−0.1536
V_{corr}^{LiH}	−0.0007	0.0014	0.0009	−0.0030
E_{int}^{LiH}	−0.2777	−0.2243	−0.2388	−0.3486
E_{bind}[b]	−0.0689	−0.0699	−0.0699	−0.0700
δ_{LiH}	0.2274	0.8002	0.5128	0.6919

[a] Atomic units are used throughout. [b] The analytical value computed with eq 31 from the total atomic and molecular energies given by the gamess code is −0.0700 hartree.

the partition) and the H atom gains that fraction of an electron. Consequently, we expect that the CT contribution to E_{def}^{Li} will be positive and on the order of $f \times$ IP, where IP is the ionization potential of Li.

Using the Q^{Li} values of Table 4 and the experimental IP of Li, we obtain for E_{def}^{Li}(CT) the values (in hartrees) 0.1747 (QTAM), 0.1387 (B-Top), 0.0797 (Mod-H), and 0.1327 (MinDef). The QTAM and B-Top numbers are reasonably close to (and smaller than) the corresponding total energy deformation values, which seems to indicate that, for Li in these two partitions, the CT effect is dominant over the effect as a result of the intrinsic charge density deformation. On the other hand, the approximation $E_{def}^{Li}(CT) = f \times IP$ is even qualitatively wrong in the MinDef partition, for this number is greater than E_{def}^{Li}. Concerning the H atom, since E_{def}^{H}(CT) has to be negative whereas the E_{def}^{H} value due to the intrinsic charge density deformation has to be positive, both quantities tend to cancel out and one should expect small total E_{def}^{H} values. The numbers in Table 4 confirm this result except in the MinDef partition, where E_{def}^{H} is too great. This is due to the kinetic energy of this atom in this partition, as shown by the ΔT^{H} value in Table 4.

Other remarkable facts relative to the intra-atomic components are the following. Most of the exchange-correlation energy is, in fact, exchange. It is interesting to remark that V_{corr}^{HH} is considerably larger (absolute value) than V_{corr}^{LiLi}. As corresponds to a positive charge for Li and a negative charge for H, $\Delta V_{ne}^{LiLi} > 0$, whereas $\Delta V_{ne}^{HH} < 0$. The contrary happens for the electron−electron repulsion; that is, $\Delta V_{ee}^{LiLi} < 0$, while $\Delta V_{ee}^{HH} > 0$.

We finally analyze the interatomic energies. We observe in Table 4 that most of the classical electrostatic energy, V_{cl}^{LiH}, can be recovered from just the point-charge term, $Q^{Li} \times Q^{H}/R_{Li-H}$. The rest of the classical interaction,[23] which collects the classical multipolar (other than charge−charge) and overlap (in the sense of ref 24) contributions, is positive in the QTAM and B-Top partitions but negative in the Mod-H and MinDef partitions. The exchange-correlation term, V_{xc}^{LiH}, correlates very well with the delocalization index, δ_{LiH}, and is very similar to the pure exchange contribution, V_{X}^{LiH}. The interatomic correlation energy, V_{corr}^{LiH} (as it also happened with the intra-atomic ones), is thus very small, in agreement with conventional wisdom. We must notice that the relative contribution of V_{cl}^{LiH} and V_{xc}^{LiH} to the total interaction energy, E_{int}^{LiH}, is very different in the four partitions. Thus, QTAM and, to a smaller degree, B-Top agree with the traditional image of ionic bonding (large and negative classical interaction with small positive contributions from overlap repulsion, here, corresponding to E_{def}). Furthermore, E_{int}^{LiH} also differs considerably in the four cases, and in the MinDef partition, this quantity is noticeably more negative than in the other three. Finally, since the binding energy, E_{bind}^{LiH}, is the same in all the cases (except for numerical errors in the integrations), it is clear that E_{int}^{LiH} and $E_{def}^{Li} + E_{def}^{H}$ contribute to E_{bind}^{LiH} in a rather different form in the four partitions.

IV. Summary and Conclusions

A molecular energy decomposition scheme based on the Li and Parr[26] partition of the nondiagonal first-order and diagonal second-order density matrices is proposed, which splits the total energy into intra-atomic and interatomic components. The method can be applied with both single-determinant (HF) or multideterminant wave functions, is independent of the details concerning the determination of the molecular wave function, and can deal equally well with different partitions of the electron density $\rho(\mathbf{r})$ into atomic contributions. Several of these partitions of $\rho(\mathbf{r})$, including the one based on the atoms provided by the quantum theory of atoms in molecules,[23] have been numerically explored by computing the energy components of H_2, N_2, and LiH molecules.

In H_2 and N_2, where electron charge transfer is absent, we have found that the relative values of the different intra-atomic and interatomic energy components are almost exclusively determined by the shape of each atomic density. Nonoverlapping atomic densities tend to give (absolute value) smaller intra-atomic and interatomic energy components than overlapping densities. The larger the overlap, the more difficult it is to recognize the original (i.e., isolated state)

atoms within molecules. In this sense, the QTAM partition, discussed in full detail in ref 23 for a representative set of molecules, is specially useful, for it provides a very appealing picture of chemical binding: atoms, relatively unchanged with respect to their in vacuo states, simply interact to form the molecule. In this partition, the atomic deformation energy is, thus, relatively small. Moreover, the large exchange-correlation interaction is the only one responsible for binding, since the total classical interaction is overall repulsive and, consequently, tends to destabilize the molecule. The image provided by the QTAM partition is certainly close to that successfully used over the years in semiempirical atomistic simulations,[44−46] in which the atomic self-energies are assumed to be approximately constant and the focus is put on the interatomic energies. Energy partitions based on strongly interpenetrating atoms tend to destroy this conventional image, as the final value of the total binding energy is the consequence of a delicate balance between intra-atomic and interatomic interactions, both of them considerably larger than the binding energy itself. We are currently applying the present energy partition method using several partitions of $\rho(\mathbf{r})$ to other homonuclear diatomics. We do not expect, however, to arrive to conclusions qualitatively different from those obtained in H_2 and N_2 molecules.

Concerning heteronuclear diatomics, the atom loosing charge has a positive and large deformation energy regardless of the partition used. This is due to both its loss of electron population and the intrinsic deformation of its atomic density with respect to the isolated state. Since both effects tend to cancel out in the negatively charged atom, it usually (but not always) has an absolute value of the deformation energy smaller than that of the positively charged atom. Contrary to homonuclear diatomics, the classical interaction energy plays a stabilizing role in the binding. Moreover, in all the partitions, most of this interaction corresponds to the point-charge interaction. The image of binding in homonuclear diatomics, almost exclusively due to the quantum-mechanical exchange-correlation interaction, is no longer valid. Here, both the classical and the pure quantum-mechanical components are relevant in understanding the binding.

Because of the existence of charge-transfer effects, a detailed comparison of the energy components obtained with different partition schemes of $\rho(\mathbf{r})$ in heteronuclear diatomics and molecules with more that two atoms is considerably more difficult than in homonuclear diatomics. To deepen our knowledge about this comparison, we are currently working on developing a sensible method to split the energy components (both intra- and interatomic) into two different contributions: a first one due to charge-transfer effects and a second one due to the intrinsic deformation of each atomic density.

Acknowledgment. Financial support from the MCyT (Project BQU2003-06553) is gratefully acknowledged.

References

(1) Fukui, K. *Acc. Chem. Res.* **1971**, *4*, 57.

(2) Fukui, K. *Theory of Orientation and Stereoselection*; Springer-Verlag: Berlin, 1975.

(3) Woodward, R. B.; Hoffmann, R. *The Conservation of Orbital Symmetry*; Verlag Chemie: Weinheim, Germany, 1970.

(4) Jeziorski, B.; Moszynski, R.; Szalewicz, K. *Chem. Rev.* **1994**, *94*, 1887.

(5) Kitaura, K.; Morokuma, K. *Int. J. Quantum Chem.* **1976**, *10*, 325.

(6) Ziegler, T.; Rauk, A. *Inorg. Chem.* **1979**, *18*, 1558; 1755.

(7) Ruedenberg, K. *Rev. Mod. Phys.* **1962**, *34*, 326.

(8) Bagus, P. S.; Hermann, K.; Bauschlicher, C. W., Jr. *J. Chem. Phys.* **1984**, *80*, 4378.

(9) Reed, A. E.; Curtiss, L. A.; Weinhold, F. *Chem. Rev.* **1988**, *88*, 899.

(10) Parr, R. G.; Yang, W. *Density-Functional Theory of Atoms and Molecules*; Oxford University Press: New York, 1989.

(11) Bader, R. F. W. *Atoms in Molecules*; Oxford University Press: Oxford, England, 1990.

(12) Glendening, E. D.; Streitwieser, A. *J. Chem. Phys.* **1994**, *100*, 2900.

(13) Day, P. N.; Jensen, J. H.; Gordon, M. S.; Webb, S. P.; Stevens, W. J.; Krauss, M.; Garmer, D.; Basch, H.; Cohen, D. *J. Chem. Phys.* **1996**, *105*, 1968.

(14) Mo, Y.; Gao, J.; Peyerimhoff, S. D. *J. Chem. Phys.* **2000**, *112*, 5530.

(15) Pophristic, V.; Goodman, L. *Nature* **2001**, *431*, 565.

(16) Bickelhaupt, F. M.; Baerends, E. J. *Rev. Comput. Chem.* **2000**, *15*, 1.

(17) Bickelhaupt, F. M.; Baerends, E. J. *Angew. Chem., Int. Ed.* **2003**, *115*, 4315.

(18) Frenking, G.; Wichmann, K.; Fröhlich, N.; Loschen, C.; Lein, M.; Frunzke, J.; Rayón, V. M. *Coord. Chem. Rev.* **2003**, *238*, 55.

(19) Salvador, P.; Mayer, I. *J. Chem. Phys.* **2004**, *120*, 5046.

(20) Mayer, I. *Chem. Phys. Lett.* **2003**, *382*, 265.

(21) Mayer, I.; Salvador, P. *Chem. Phys. Lett.* **2003**, *383*, 368.

(22) Alcoba, D. R.; Torre, A.; Lain, L.; Bochicchio, R. C. *J. Chem. Phys.* **2005**, *122*, 074102.

(23) Blanco, M. A.; Martín Pendás, A.; Francisco, E. *J. Chem. Theory Comput.* **2005**, *1*, 1096.

(24) Martín Pendás, A.; Blanco, M. A.; Francisco, E. *J. Chem. Phys.* **2004**, *120*, 4581.

(25) Martín Pendás, A.; Francisco, E.; Blanco, M. A. *J. Comput. Chem.* **2004**, *26*, 344.

(26) Li, L.; Parr, R. G. *J. Chem. Phys.* **1986**, *84*, 1704.

(27) McWeeny, R. *Methods of Molecular Quantum Mechanics*, 2nd ed.; Academic Press: London, 1992.

(28) Baerends, E. J.; Gritsenko, O. V. *J. Phys. Chem. A* **1997**, *101*, 5383.

(29) Hirshfeld, F. L. *Theor. Chim. Acta* **1977**, *44*, 129.

(30) Rico, J. F.; López, R.; Ramírez, G. *J. Chem. Phys.* **1999**, *110*, 4213.

(31) Bader, R. F. W.; Beddall, P. M. *J. Chem. Phys.* **1972**, *56*, 3320.

(32) Bader, R. F. W. *Monatsh. Chem.* **2005**, *136*, 819.

(33) Kullback, K.; Leibler, R. A. *Ann. Math. Stat.* **1951**, *22*, 79.

(34) Becke, A. D. *J. Chem. Phys.* **1988**, *88*, 2547.

(35) Popelier, P. L. A.; Kosov, D. S. *J. Chem. Phys.* **2001**, *114*, 6539.

(36) Popelier, P. L. A.; Kosov, D. S. *J. Chem. Phys.* **2000**, *113*, 3969.

(37) Popelier, P. L. A.; Jouber, L.; Kosov, D. S. *J. Phys. Chem. A* **2001**, *105*, 9254.

(38) Schmidt, M. W.; Baldridge, K. K.; Boatz, J. A.; Elbert, S. T.; Gordon, M. S.; Jensen, J. H.; Koseki, S.; Matsunaga, N.; Nguyen, K. A.; Su, S. J.; Windus, T. L.; Dupuis, M.; Montgomery, J. A. *J. Comput. Chem.* **1993**, *14*, 1347.

(39) Koga, T.; Watanabe, S.; Kanayama, K.; Yasuda, R.; Thakkar, A. J. *J. Chem. Phys.* **1995**, *103*, 3000.

(40) Guerra, C. F.; Handgraaf, J. W.; Baerends, E. J.; Bickelhaupt, F. M. *J. Comput. Chem.* **2003**, *25*, 189.

(41) Nalewajski, R. F.; Parr, R. G. *Proc. Natl. Acad. Sci.* **2000**, *97*, 8879.

(42) Nalewajski, R. F.; Parr, R. G. *J. Phys. Chem. A.* **2001**, *105*, 7391.

(43) Parr, R. G.; Ayers, P. W.; Nalewajski, R. F. *J. Phys. Chem. A.* **2005**, *109*, 3957.

(44) Born, M.; Huang, K. *Dynamical Theory of Crystal Lattices*; Oxford University Press: Oxford, England, 1954.

(45) Hirschfelder, J. O.; Curtis, C. F.; Bird, R. B. *Molecular Theory of Gases and Liquids*; Wiley: New York, 1954.

(46) Allen, M. P.; Tildesley, D. J. *Computer Simulation of Liquids*; Clarendon Press: Oxford, England, 1987.

CT0502209